

Dimensional complexity and spectral properties of the human sleep EEG

Y. Shen^a, E. Olbrich^{a,*}, P. Achermann^b, P.F. Meier^a

^aPhysics Institute, University of Zurich, CH-8057 Zurich, Switzerland

^bInstitute of Pharmacology and Toxicology, University of Zurich, CH-8057 Zurich, Switzerland

Accepted 11 October 2002

Abstract

Objective: The relevance of the dimensional complexity (DC) for the analysis of sleep EEG data is investigated and compared to linear measures.

Methods: We calculated DC of artifact-free 1 min segments of all-night sleep EEG recordings of 4 healthy young subjects. Non-linearity was tested by comparing with DC values of surrogate data. Linear properties of the segments were characterized by estimating the self-similarity exponent α based on the detrended fluctuation analysis which quantifies the persistence of the signal and by calculating spectral power in the delta, theta, alpha and sigma bands, respectively.

Results: We found weak nonlinear signatures in all sleep stages, but most pronounced in sleep stage 2. Strong correlations between DC and linear measures were established for the self-similarity exponent α and delta power, respectively.

Conclusions: The dimensional complexity of the sleep EEG is influenced by both linear and nonlinear features. It cannot be directly interpreted as a nonlinear synchronization measure of brain activity, but yields valuable information when combined with the analysis of linear measures.

© 2002 Elsevier Science Ireland Ltd. All rights reserved.

Keywords: Self-similarity exponent; Spectral power; Nonlinear analysis; Surrogate analysis

1. Introduction

First attempts to apply methods from nonlinear time series analysis to electroencephalograms (EEG) were carried out in the framework of the chaos hypothesis, i.e. it was assumed that the EEG within a particular psychophysiological state could be described by a deterministic chaotic system and therefore could be characterized by invariant measures such as the fractal dimension of the corresponding attractor or as the Lyapunov exponents. In the case of sleep EEG the sleep stages were considered as distinct psychophysiological states.

One of the first publications in this framework was by Babloyantz et al. (1985). They applied the Grassberger-Procaccia (GP) algorithm (Grassberger and Procaccia, 1983a,b) for the determination of the correlation dimension to time series of sleep EEG segments. They reported decreasing correlation dimensions from REM sleep to sleep stage 2 to slow wave sleep. Since then numerous studies appeared confirming this result on larger samples and with different data sets (Ehlers et al., 1991; Röschke

and Aldenhoff, 1991; Achermann et al., 1994b; Pradhan et al., 1995). In addition to low correlation dimensions also positive Lyapunov exponents have been reported (Fell et al., 1993), indicating that the EEG may result from a low-dimensional chaotic process.

Dimension analysis in the framework of the chaos hypothesis was not only applied to characterize the sleep EEG, but to all kinds of psychophysiological conditions in normal as well as pathological states.

Already from the beginning these results have been questioned for several reasons: From a general point of view it seems very unlikely that such a complex system as the brain should produce an activity which can be described by low-dimensional dynamics. Moreover, if the existence of a sufficiently low-dimensional attractor is assumed, then for a reliable estimate of the fractal dimension a time series has to fulfill requirements such as stationarity, a sufficiently large number of data points and a reasonable signal to noise ratio (see e.g. Kantz and Schreiber, 1997). It is very unlikely that these requirements are simultaneously met in the case of the EEG.

Moreover, the interpretation of low values of the correlation dimension as a sign of deterministic chaos has been challenged by Osborne and Provenzale (1989): they showed

* Corresponding author. Tel.: +41-1-635-4585; fax: +41-1-635-5704.
E-mail address: olbrich@physik.unizh.ch (E. Olbrich).

that correlated noise exhibiting power law spectra $P(f) \propto f^{-\beta}$, may result in low values of the correlation dimension. Furthermore, Rapp et al. (1993) applied a low-pass filter to white noise and showed that the resulting time series produced low correlation dimensions. These studies demonstrated that spurious low correlation dimensions may already result from linear stochastic processes. To avoid these spurious estimates, Theiler (1986) proposed a correction to the original GP algorithm, which reduces the effects of linear correlations. He showed that with this correction the scaling regions that lead to low dimensions for colored noise such as presented by Osborne and Provenzale (1989) disappeared. A first application of this correction to EEG data was reported by Theiler and Rapp (1996). They re-examined a set of human EEG data recorded during rest and while performing simple tasks which has previously been reported to exhibit low values of the correlation dimension. Using this correction, the scaling region was reduced or disappeared totally, leading the authors to conclude that no convincing evidence for low-dimensional behavior could be found. A similar result was obtained by Schreiber (1999) for a data set used for epileptic seizure prediction by Elger and Lehnertz (1998).

Many authors dropped the chaos hypothesis and referred to their dimension estimates not as an absolute measure of a fractal dimension of a strange attractor but as a relative measure of dimensional complexity (see e.g. Pritchard and Duke, 1992; Rey and Guillemant, 1997, and references therein). However, without referring to an attractor dimension the interpretation of the dimensional complexity turned out to be equivocal.

The present work focuses on two problems: First, to what extent does the dimensional complexity (DC) really measure nonlinear properties in sleep EEG? This question is related to the more general problem of nonlinearity in the sleep EEG. To answer it we compared DC of the original data with those of surrogate data, i.e. time series which resemble the linear properties and the amplitude distribution of the original time series, but are otherwise random (see Theiler et al., 1992; Schreiber and Schmitz, 2000, and references therein). Second, we studied the relationship between different spectral features and DC in order to identify those spectral features which have the largest impact on the DC.

2. Materials and methods

2.1. EEG data

The sleep EEG of 4 healthy young right handed males (aged 23–25 years) was analyzed. The data are 8-h baseline recordings (23:00–07:00 h) of a previous study (Endo et al., 1998) performed in the sleep laboratory of the Institute of Pharmacology and Toxicology, University of Zurich. The EEG signals from the C₃-A₂ derivation were conditioned by the following analog filters: a high-pass filter (−3 dB at 0.16

Hz), a low-pass filter (−3 dB at 102 Hz, < −40 dB at 256 Hz), and a notch filter (50 Hz). The data were sampled with a frequency of 512 Hz, digitally filtered (low-pass FIR filter, −3 dB at 49 Hz), and stored on a PC with a resolution of 128 Hz, i.e. the sampling time is $\Delta = 1/128$ s.

Sleep stages were visually scored for 20 s epochs according to criteria of Rechtschaffen and Kales (1968). Three hundred and sixty-one segments with a duration of 1 min (7680 points) were selected after visual inspection for lack of obvious nonstationarity due to artifacts and arousals. Only 1 min segments containing a definite sleep stage (REM sleep, stage 2 or slow-wave sleep (SWS, stage 3 and 4)) were considered. There was only a very small number of artifact-free 1 min segments from sleep stage 1. Thus we did not include segments from this sleep stage in the further analysis.

For each 1 min EEG segment 39 surrogate data sets were generated, using the method of Schreiber and Schmitz (1996), so that the resulting surrogate time series had exactly the same amplitude distribution as the original time series and almost the same power spectrum. We checked the influence of choosing the exact power spectrum instead of the exact distribution, as recommended by Kugiumtzis (1999) but found only marginal differences.

2.2. Dimensional complexity (DC)

DC is based on the correlation dimension, which can be estimated by using the GP-algorithm: If one has a sample of N state-vectors \vec{X}_i from the attractor, one can calculate the correlation sum

$$C(r) = \frac{2}{(N-W)(N-1-W)} \sum_{i=1}^N \sum_{j=i+1+W}^N \Theta(r - \|\vec{X}_i - \vec{X}_j\|) \quad (1)$$

where Θ is the Heaviside step function and $\|\cdot\|$ is chosen to be the maximum norm, L_∞ . W denotes the Theiler correction (Theiler, 1986).

Given a time series, e.g. a segment of one channel of EEG data, say $\{x_1, \dots, x_i, \dots, x_N\}$, a phase space is reconstructed by building m -dimensional vectors

$$\vec{X}_i = (x_i, x_{i-n_\tau}, x_{i-2n_\tau}, \dots, x_{i-(m-1)n_\tau})$$

with $i = 1 + (m-1)n_\tau, \dots, N$. This procedure is called delay embedding; $\tau = n_\tau \Delta$ denotes the delay time and m the embedding dimension. The correlation dimension D_2 is defined as

$$D_2(r) = \frac{d \log C(r)}{d \log r} \quad D_2 := \lim_{r \rightarrow 0} D_2(r) \quad (2)$$

In practice, due to the finite amount of data, the limit cannot be performed, but if $D_2(r) \approx \text{const}$ on length scales smaller than some length scale r_0 , D_2 is determined by extrapolating this behavior to $r \rightarrow 0$. In the presence of noise this plateau will be restricted to a finite region, the so-called scaling

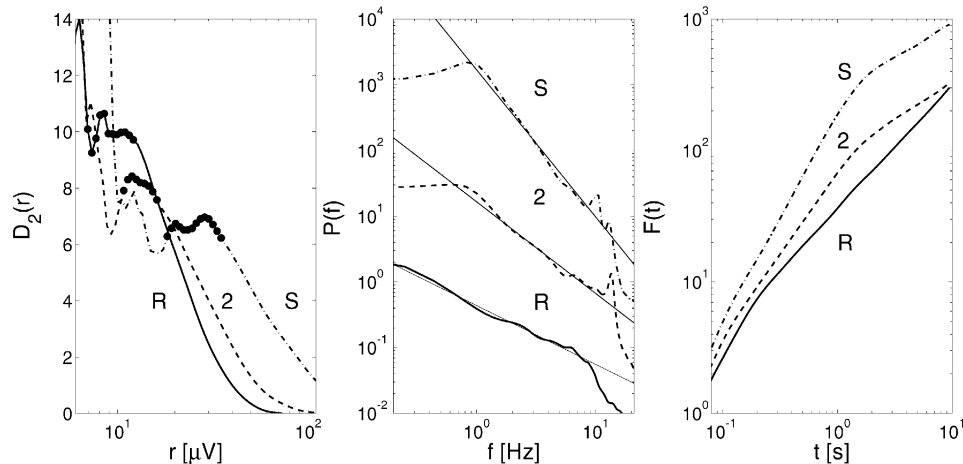


Fig. 1. Correlation dimension $D_2(r)$ using embedding dimension $m = 20$, delay time $\tau = 3\Delta$ ($\Delta = 1/128$ s) and Theiler correction $W = 1\Delta$ (left panel), spectral power $P(f)$ (middle panel) and the detrended fluctuation function $F(t)$ (right panel) for 3 selected EEG segments of 60 s duration representative for REM sleep (R), sleep stage 2 (2) and slow-wave sleep (S). To avoid superposition of the curves, the power spectra of stage 2 and REM sleep were displaced downwards by one decade and two decades, respectively. The filled circles in the left panel denote the automatically determined plateaus. The straight lines in the middle panel represent the best linear fit within the scaling range.

region $r_0 \geq r \geq r_{\text{noise}}$, where r_{noise} is related to the amplitude of the noise.

A short plateau can be detected in the $D_2(r)$ curve of EEG signals for an appropriate combination of small values of delay time τ and Theiler correction W . Such kind of plateaus resemble the picture of noisy deterministic chaotic systems. This has been reported in earlier studies (Lehnertz and Elger, 1995; Besthorn et al., 1995; Schmid and Dünki, 1996; Tirsch et al., 2000). We note, however, that the Theiler corrections used were too small to remove temporal correlations in EEG signals entirely. When applying sufficiently large W value, the plateau will disappear. Consequently, the D_2 values estimated with small W are very likely not the correlation dimensions of chaotic attractors and thus are often referred as dimensional complexity (DC). DC is often estimated by an automatic plateau extraction. In the present study, the optimal values for the parameters m , τ and W were chosen in such a way that a plateau as large as possible was obtained. In addition, the DC value should remain constant, when the embedding dimension m deviates slightly from its optimal value. Taking both criteria into account, the optimal parameter set (m , τ , W) for scalp sleep EEG recordings was determined as (20, 3Δ , 1Δ). In the left panel of Fig. 1, the $D_2(r)$ curves for the chosen parameter set were plotted for 3 selected EEG segments representative for REM sleep, stage 2 and slow-wave sleep. For further details of the algorithm see Appendix A.

2.3. Estimation of the self-similarity exponent α

The power spectrum $P(f)$ of the EEG segments shows very often a power law behavior, i.e. $P(f) \propto f^{-\beta}$. For the examples discussed above their power law spectra are demonstrated in the middle panel of Fig. 1. This indicates that the EEG signal may exhibit self-similarity within a

certain range of time scales. For a description of self-similarity we refer to Appendix B. Furthermore, the β exponent describes the roughness of the time series, which is also often termed as persistence. In this study we applied a recently proposed method, called detrended fluctuation analysis (DFA) (Peng et al., 1994), to analyze persistence in EEG signals. The fluctuation function $F(t)$ measures the fluctuations of EEG signals around the local trend within consecutive time windows of length t . The definition of $F(t)$ is given in Appendix B. In the present study, linear trends in EEG signals were taken into account. For a self-similar time series, $F(t)$ can be approximated by the power law

$$F(t) \propto t^\alpha \quad (3)$$

where α is the so-called self-similarity exponent. The fluctuation function and the power spectrum are related by (Viswanathan et al., 1997)

$$F^2(t) \propto \int_{1/t}^{\infty} \frac{P(f)}{f^2} df \quad (4)$$

Thus, the relationship between the exponents α and β is given by

$$\alpha = (\beta + 1)/2 \quad (5)$$

In the right panel of Fig. 1 the detrended fluctuation functions $F(t)$ are shown for the same 3 EEG-segments. For the segments of stage 2 and slow-wave sleep a linear scaling behavior in the double logarithmic representation is seen, which extends from 0.1 s up to 1 s. In the case of REM sleep one distinguishes a scaling region that extends from 0.2 s up to 10 s. The observed scaling behaviors are typical for the sleep stages. In the present study, we used the α -exponents determined from the scaling range [0.2 s 1 s] to characterize different degree of persistence in EEG signals recorded during different sleep stages.

It should be emphasized that our α -estimation was not influenced by frequency cutoffs. The discreteness of the investigated time series implied an effective high-frequency cutoff at the sampling rate 64 Hz or $(0.016 \text{ s})^{-1}$, which is far below the lower bound of our scaling region. Moreover, we have simulated the influence of low-frequency cutoff on the detrended fluctuation functions with a time series of colored noise. This time series was conditioned by the same filter as in the case of EEG-signals, namely -3 dB at 0.16 Hz or $(6 \text{ s})^{-1}$. We found that $F(t)$ of the filtered signal does not deviate from that of the unfiltered one in the range where we estimated α -exponents.

2.4. Estimation of spectral power

We estimated the power spectral density (PSD) using the Yule–Walker method based on autoregressive (AR)-modeling. A 64th-order AR-model was computed on 1 min EEG segments. The power in a frequency range $[f_{\min}, f_{\max}]$ was estimated by

$$P = \sum_{f_{\min} \leq f \leq f_{\max}} P(f) \cdot \Delta f \quad (6)$$

We used the following frequency bands: delta (0.5–4 Hz), theta (4–8 Hz), alpha (8–12 Hz) and sigma (12–16 Hz).

2.5. Statistical analysis

We used the Spearman rank-order correlation coefficient r_s (Press et al., 1992) to quantify the relationship between two different characteristics, for example between DC and the self-similarity exponent α . The significance P for a r_s value is the probability of observing the r_s value under the null hypothesis that the different measured characteristics are not correlated. This null hypothesis will be rejected, if P for a r_s value is smaller than 0.05.

3. Results

Fig. 2 shows the sleep profile and the time courses of different measures for one all-night EEG. The averaged DC of the surrogate data is denoted by $\langle DC^{\text{surrt}} \rangle$, while in the following the dimensional complexity of the original segment is labeled DC . The EEG recording was subdivided into consecutive, non-overlapping epochs of 1 min duration. The curves of all 4 EEG measures exhibit cyclic changes which coincide with the non-REM/REM sleep cycles. When P_δ and α are of highest values during stage 4, both DC and $\langle DC^{\text{surrt}} \rangle$ attain the lowest levels. In contrast, the values of P_δ and α are lowest during REM sleep, while the DC and $\langle DC^{\text{surrt}} \rangle$ reach the highest levels. For DC and $\langle DC^{\text{surrt}} \rangle$, we observed a large similarity in their temporal evolution in the course of sleep.

To exclude effects of artifacts and obvious nonstationarities we selected 363 segments of 1 min duration each for further investigation. For 297 of them, a DC value could be

estimated (see Appendix A). These segments were divided into 4 groups: REM sleep, slow-wave sleep (stages 3 and 4) and two groups of stage 2. One group, called 2A, consists of segments with sharp waves larger than $100 \mu\text{V}$, which correspond to vertex waves and K-complexes, while the second group 2B comprises segments with only small or no sharp waves. Hence, the EEG segments of the group 2A are obviously nonstationary. We took, however, these segments into consideration, since the vertex waves and K-complexes are typical features of EEG signals during stage 2. Note that sleep spindles can be observed in both 2A and 2B. Due to the lack of suitable segments from sleep stage 1, non-REM sleep in this paper is related only to sleep stage 2 and slow-wave sleep. The numbers of segments with a reliable DC of each group, n^{eff} , together with the respective total number, n^{tot} , are given in Table 1 as well as an overview of different other measures. Only n^{eff} segments from each group contributed to the averages.

To detect nonlinearities hidden in the EEG signals we compared the DC values of the original data and those of the corresponding surrogate data. The significance S for testing nonlinearity is defined by

$$S = \frac{|\langle DC^{\text{surrt}} \rangle - DC|}{\sigma(DC^{\text{surrt}})} \quad (7)$$

$\langle DC^{\text{surrt}} \rangle$ denotes the mean value of DC of the surrogate data and $\sigma(DC^{\text{surrt}})$ its standard deviation. If the value of S was larger than 1.96, the original signal was considered nonlinear (with a 0.95 level of significance). The mean values of the relative difference between DC and $\langle DC^{\text{surrt}} \rangle$, Δ^{rel} , the percentage of segments with $\langle DC^{\text{surrt}} \rangle > DC$, n^{rel} , and the mean values of $\sigma(DC^{\text{surrt}})$ are reported in Table 2.

The preset significance level defines the probability for the test to reject the null hypothesis (i.e. linear stochastic system) for a single segment although it is actually true. For a larger set of tests one would expect a false rejection rate of 5% if the significance level is set to 0.95 and the null hypothesis is true.

In a first step we tested whether our surrogate data were well constructed, i.e. fulfilling the null hypothesis, by performing the surrogate data test on one surrogate data set itself for each original segment. This strategy to use surrogate surrogate data was proposed by Theiler and Prichard (1997). The mean value of the significance (7) for each group of these data is denoted by \bar{S}^c and is also displayed in Table 2. The values of \bar{S}^c near the theoretical value $\sqrt{2/\pi} \approx 0.79$ together with a rate of false rejections $n_{S > 1.96}$ smaller than 5% ascertain that the surrogate data we used for detecting nonlinearity actually fulfill the null hypothesis for the segments from REM sleep and 2B. In the case of SWS and stage 2A the rejection rate slightly exceeded 5%.

The percentage of EEG segments where the null hypothesis of linearity had to be rejected varies from 13.9% for REM sleep to 61.8% in group 2B, clearly exceeding the 5% of possible false rejections. This means that there are segments

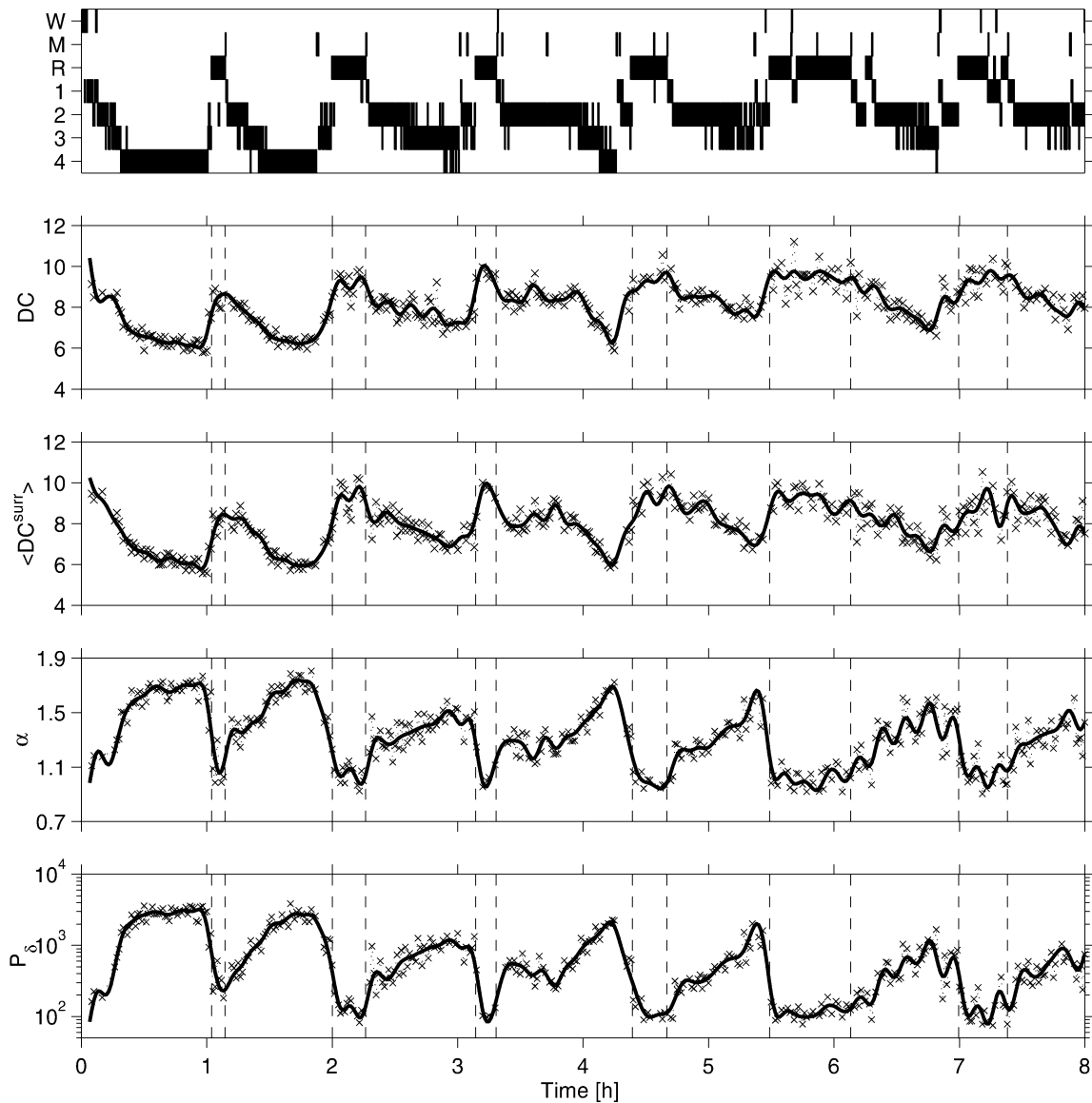


Fig. 2. Vigilance states (W, waking; M, movement time; R, REM sleep; 1–4, non-REM sleep stages 1–4), dimensional complexity of original data DC , dimensional complexity of surrogate data $\langle DC^{surr} \rangle$, self-similarity exponent α and delta power P_{δ} plotted for an all-night sleep EEG recording (from top to bottom). The values are plotted for 1 min epochs, except for sleep stages which were determined for 20 s epochs. For clarity, we plotted the smoothed curves together with the original data which are represented by the symbols \times . The curves were smoothed by a 4th-order low-pass Butterworth filter with cutoff frequency 0.0067 Hz. Vertical dashed lines delineate REM sleep episodes.

Table 1

The number of segments computed, n^{tot} , the number of segments with a reliable value of DC, n^{eff} , and the group means \pm SD for DC, $\langle DC^{surr} \rangle$, α -exponent and \log_{10} delta power P_{δ} ^a

Stage	n^{tot}	n^{eff}	DC	$\langle DC^{surr} \rangle$	α	$\log_{10} P_{\delta}$
SWS	122	111	6.78 ± 0.74	6.85 ± 0.69	1.59 ± 0.12	3.27 ± 0.21
2A	90	82	8.88 ± 0.63	8.69 ± 0.66	1.29 ± 0.12	2.63 ± 0.17
2B	94	68	9.13 ± 0.61	10.12 ± 0.87	1.11 ± 0.10	2.26 ± 0.18
REMS	57	36	9.82 ± 0.41	10.33 ± 0.67	0.99 ± 0.07	1.93 ± 0.12

^a The EEG segments were divided into 4 groups: slow-wave sleep (SWS), stage 2 group A (2A), stage 2 group B (2B) and REM sleep (REMS) (see text).

Table 2

Percentage of segments with $\langle DC^{surr} \rangle > DC$; n^{rel} ; Spearman correlation coefficient r_S between $\langle DC^{surr} \rangle$ and DC ; mean values of relative difference between $\langle DC^{surr} \rangle$ and DC ; $\Delta^{rel} = (\langle DC^{surr} \rangle - DC)/DC$; mean values of $\sigma(DC^{surr})$; mean values of the significance S ; percentage of segments with $S > 1.96$, $n_{S>1.96}$; mean values of the significance S^c for control data (see text); and percentage of control data with $S^c > 1.96$, $n_{S^c>1.96}$

Stage	n^{rel}	r_S	Δ^{rel}	$\overline{\sigma(DC^{surr})}$	\bar{S}	$n_{S>1.96}$	\bar{S}^c	$n_{S^c>1.96}$
SWS	59%	0.89	1%	0.23	1.12	15.3%	0.91	7.2%
2A	37%	0.60	-2%	0.36	1.42	26.8%	0.75	7.3%
2B	93%	0.53	11%	0.50	2.20	61.8%	0.63	4.4%
REMS	89%	0.80	3%	0.60	0.98	13.9%	0.72	2.8%

in all 4 groups, for which the model of a linear stochastic system is not sufficient and nonlinearity has to be taken into account. The strongest effects were found in sleep stage 2.

To illustrate the distribution of nonlinearity we plotted the values of $\langle DC^{surr} \rangle$ against DC in Fig. 3. It is seen that the data points for segments of slow-wave sleep are distributed closely along the line $DC = \langle DC^{surr} \rangle$ and almost uniformly on both sides of the line. In contrast, the data points for segments of group 2A lie mostly below the line. We found also that almost all data points of segments from REM sleep and group 2B are situated above the line.

However, the $\langle DC^{surr} \rangle$ are significantly larger than DC only for the segments of group 2B.

The group mean of S , the fraction of segments with $S > 1.96$ and the Spearman correlation coefficient r_S between $\langle DC^{surr} \rangle$ and DC are also given in Table 2. Note that $\langle DC^{surr} \rangle$ and DC are strongly correlated in SWS and REM sleep. This finding indicates that the DC values mainly reflect the linear properties of EEG signals during REM sleep and slow-wave sleep. However, for the majority of the segments of group 2B the S value is larger than 1.96 and also the mean value of S is larger than the threshold value. This fact indicates the signature for nonlinearity in EEG segments of stage 2 without K-complexes. By visual inspection of the corresponding EEG segments, we observed the almost periodic occurrence of spindles (Achermann and Borbély, 1997). The power spectrum of these segments exhibits a pronounced peak in the sigma range i.e. [12 Hz, 14 Hz]. In the surrogate data segments, the spindles disappear, while the power spectrum of the whole segment is preserved and therefore still shows this peak. This means that sigma activity spreads over the whole segment. Therefore, we ascribe the signature of nonlinearity to temporally organized spindle activities.

Furthermore, a considerable number of segments of

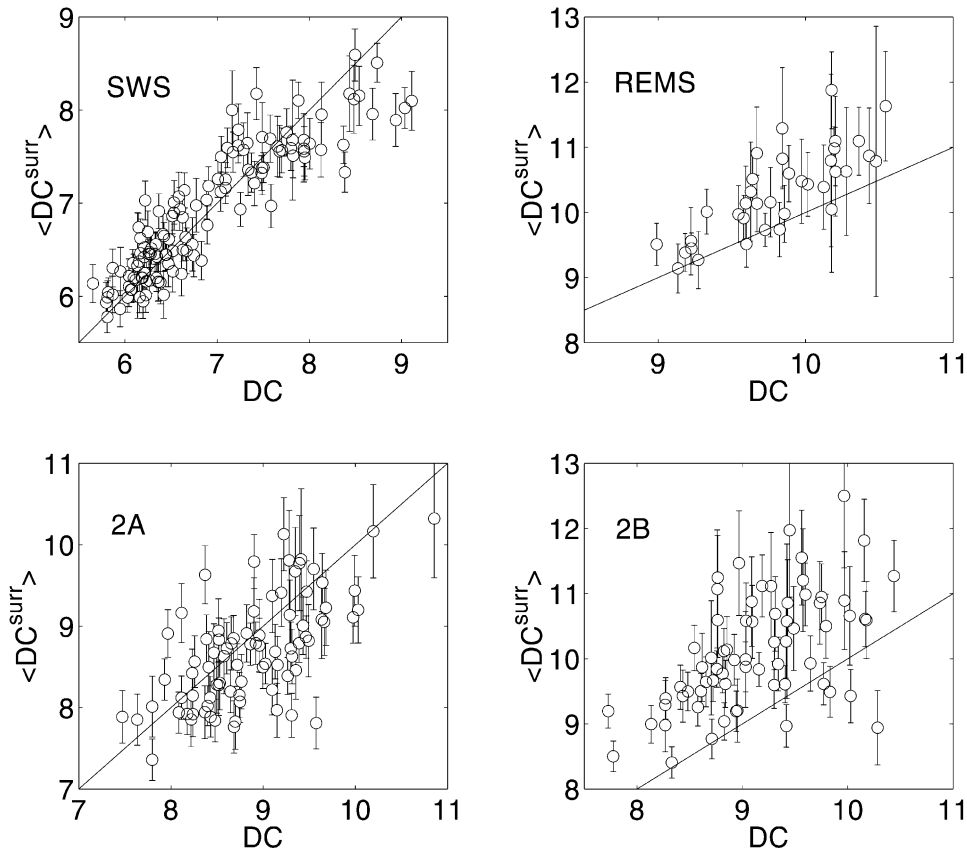


Fig. 3. Comparison of DC values for each EEG segment of different groups, DC , and the mean value of DC for its surrogates, $\langle DC^{surr} \rangle$. The vertical error bars denote the standard deviation of DC values of the surrogates. A data point above the straight line indicates that the DC value for this segment is lower than the value of $\langle DC^{surr} \rangle$ and vice versa.

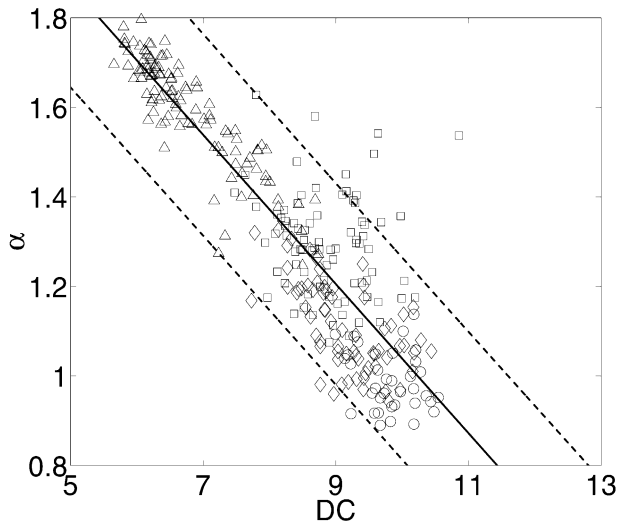


Fig. 4. Self-similarity exponent α vs. DC for slow-wave sleep (Δ), stage 2 group A (\square), stage 2 group B (\diamond) and REM sleep (\circ). The straight line denotes the best linear fit and the pair of dashed lines indicates the 95% prediction interval.

group 2A has also an S value larger than 1.96. In contrast to 2B, most of them have a larger DC than $\langle DC^{surr} \rangle$. This observation can be attributed to the nonstationarity in EEG-signals due to the occurrence of K-complexes. To investigate their influence on DC and $\langle DC^{surr} \rangle$ we performed simulations with colored noise, showing power law spectra similar to the EEG, in which K-complexes were introduced artificially. They showed that the DC estimates are barely influenced whereas the $\langle DC^{surr} \rangle$ values are considerably reduced.

Note that in the segments of group 2A also spindle activity occurs. Therefore the spindles and the K-complexes have opposite effects on the difference between DC and $\langle DC^{surr} \rangle$, which might be the reason for the difference between the rejection rates ($n_{S>1.96}$ in Table 2) in groups 2A and 2B.

Despite of the sign for nonlinearity the values of DC for segments of both groups in sleep stage 2 are still correlated significantly with those of $\langle DC^{surr} \rangle$. In summary, a pronounced sign for nonlinearity was found only during sleep stage 2. However, the part of the fluctuations of DC

Table 3

The Spearman correlation coefficient r_S between DC , α -exponent and different power bands: delta power P_δ , theta power P_θ , alpha power P_α , and sigma power P_σ ^a

Stage	(DC, α)	(DC, P_δ)	(DC, P_θ)	(DC, P_α)	(DC, P_σ)
SWS	-0.87**	-0.78**	-0.33**	0.52**	0.24*
2A	-0.18	-0.35**	-0.32**	0.14	-0.18
2B	-0.62**	-0.54**	-0.09	-0.01	-0.16
REMS	-0.18	-0.42*	-0.43*	0.14**	0.32
Non-REMS	-0.85**	-0.86**	-0.72**	-0.34**	0.44**
All stages	-0.87**	-0.88**	-0.76**	-0.49**	0.04

^a Note that non-REM sleep comprises stages 2, 3 and 4. Asterisks denote that these r_S values are statistically significant, ** $P < 0.01$ and * $P < 0.05$.

which is connected with nonlinear effects varies from 1% in slow-wave sleep to maximal 11% in group 2B (see Δ^{rel} in Table 2) leading to the conclusion that there is only weak nonlinearity in sleep EEG data.

Next, we focused on the relationship between DC and various linear measures. The self-similarity exponent α exhibited a negative correlation with DC (Fig. 4). Taking (DC , α) points of all sleep stages into consideration, the Spearman rank coefficient r_S yielded a value of -0.87. However, the correlations differed between the sleep stages (see Table 3). A strong negative correlation ($r_S = -0.87$) between DC and α prevailed within slow-wave sleep. A negative correlation was also evident within stage 2 group B ($r_S = -0.62$). This means that weak nonlinearity and a correlation between DC and a linear measure are not mutually exclusive in this group. In contrast, in stage 2A there were no significant correlations between DC and α . As mentioned above, DC seems not to be sensitive to the occurrence of infrequent sharp waves contrary to strong influence on the α exponent revealed by the same simulations using colored noise. Also for REM sleep the correlation between α and DC was not significant.

Finally, we also investigated the relationship between DC and the spectral power in different frequency bands (Fig. 5). A negative correlation between DC and power in the low-frequency bands in the delta ($r_S = -0.88$) and theta range ($r_S = -0.76$) was observed. Negative correlations were still present within the different sleep stages (Table 3). As an exception we found a clear positive correlation ($r_S = 0.52$) between DC and log alpha power in slow-wave sleep. However, when taking all stages into consideration, the correlation is negative ($r_S = -0.49$). A positive correlation between DC and sigma power within non-REM sleep ($r_S = -0.44$) and slow-wave sleep was observed (Fig. 5 and Table 3).

To estimate the contribution of the single frequency bands to the overall variation of DC , we have to bear in mind that the different bands may be correlated. Therefore, we performed a multiple linear regression with DC as a response and the log power in delta (P_δ), theta (P_θ), alpha (P_α), sigma (P_σ) range as a group of predictor variables. Variables have been normalized with respect to their standard deviations $\sigma(\cdot)$ so that the resulting coefficients are comparable with correlation coefficients.

We found the following relationship within non-REM sleep

$$\frac{DC}{\sigma(DC)} = -0.97(\pm 0.11) \cdot \frac{\log P_\delta}{\sigma(\log P_\delta)} - 0.02(\pm 0.11) \cdot \frac{\log P_\theta}{\sigma(\log P_\theta)} + 0.22(\pm 0.07) \cdot \frac{\log P_\alpha}{\sigma(\log P_\alpha)} + 0.03(\pm 0.06) \cdot \frac{\log P_\sigma}{\sigma(\log P_\sigma)} + 10.68(\pm 0.79)$$

In brackets, the 95% confidence interval for each coefficient is given. Significant is only the negative correlation between DC and delta power, together with the positive correlation between DC and alpha power. Furthermore, we also found a positive overall correlation between the exponent α and

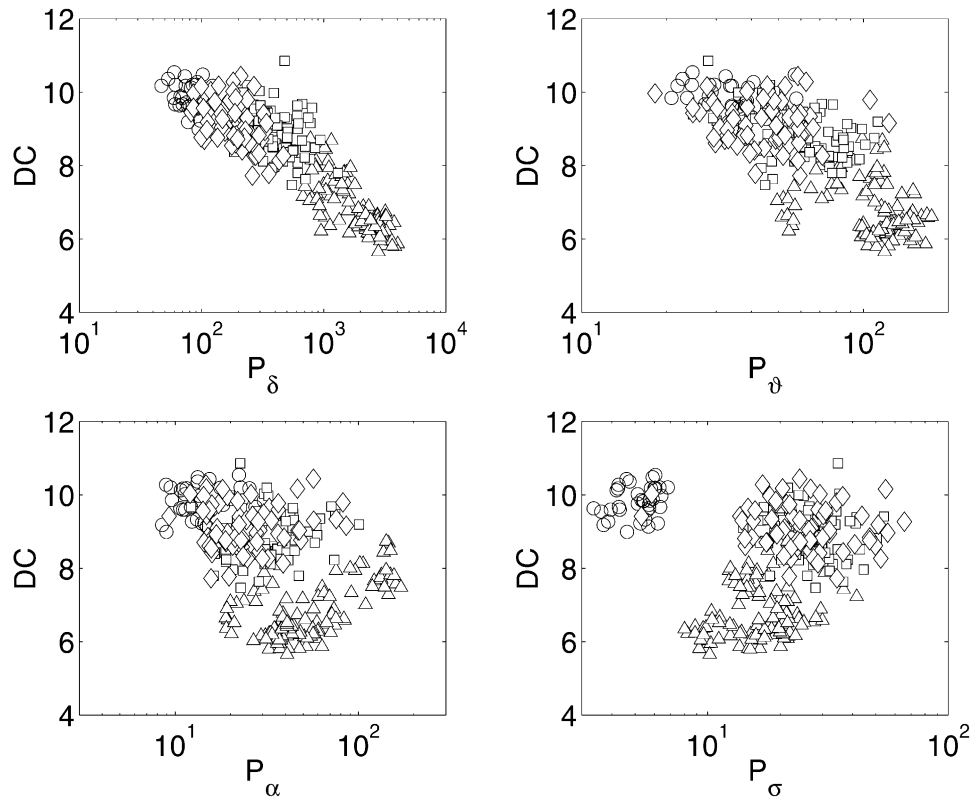


Fig. 5. DC vs. power in different frequency bands (delta power in upper left panel, theta power in upper right panel, alpha power in lower left panel and sigma power in lower right panel.). Symbols as in Fig. 4.

delta power, $r_S = 0.96$, and a negative correlation between the exponent α and alpha power within slow-wave sleep, $r_S = -0.40$. Therefore, the relation between α and the power bands reflects the relation between DC and α .

4. Discussion

Our analysis showed that the variations of the dimensional complexity (DC) of the sleep EEG in the course of a night can be explained to a large extent by linear properties of the EEG time series. The surrogate data analysis revealed only weak differences between DC values of the original data and their surrogates. In sleep stage 2 only, we found a considerable number of segments with a nonlinear signature. We were able to identify two distinct processes which are responsible for these nonlinear signatures: The occurrence of sharp waves, i.e. K-complexes, decreased DC of the surrogates, but did not affect DC of the original data, while the segments without large sharp waves showed a lower DC compared to the surrogates. The disappearance of the sleep spindles in the surrogate data indicates that the second signature is caused by the regular occurrence of the spindle activity (Achermann and Borbély, 1997). This interpretation needs further investigation. A related hypothesis was raised in a recent publication of Ferri et al., 2002, in

which the nonlinear signature was related to the arousal phases of the cyclic alternating pattern (CAP).

We have to mention at this point that not only nonlinearity causes a rejection of the null hypothesis of a linear stochastic system but also nonstationarity. Therefore one could argue that the occurrence of sleep spindles and K-complexes should be related rather to nonstationarity than to nonlinearity. While in principle this objection is justified we decided to use only the notion of nonlinearity because from a time series analysis point of view the distinction between nonlinearity and nonstationarity is not unique. A nonstationary linear process can be rewritten as a stationary nonlinear process by extending the state space.

Our general result of ‘weak nonlinearity’ of the sleep EEG is in agreement with previous studies (Achermann et al., 1994a; Fell et al., 1996; Pereda et al., 1998). However, the surrogate analysis within single sleep stages showed some differences to earlier investigations (Achermann et al., 1994a; Pereda et al., 1998). Achermann et al. (1994b) reported for all sleep stages a slightly higher DC of the surrogates, significant for stage 2 and slow-wave sleep. Pereda et al. found significant differences in slow-wave sleep. Contrary to these findings we found significant nonlinearity only in stage 2. This discrepancy may be due to two reasons: We used the iterated amplitude adjusted surrogates compared to purely phase randomized surrogates (Acher-

mann et al., 1994a) or amplitude adjusted phase randomized surrogates (Pereda et al., 1998). Second, in both previous studies (Achermann et al., 1994a; Pereda et al., 1998) DC was estimated by using Takens estimator compared to the automatic plateau detection, which was employed in the present study. It should be noted that using other nonlinear measures than DC for the surrogate test, such as mutual information or nonlinear prediction errors one may detect different nonlinear signatures.

The surrogate data test revealed strong correlations between DC of original and surrogate data indicating that a large part of variation of DC is due to linear properties. In particular, strong negative correlations between α and DC and between P_δ and DC were observed. These correlations were most pronounced in slow-wave sleep and less so in sleep stage 2, except for some segments from group 2A. The aberrant segments contain K-complexes. The occurrence of K-complexes in a segment does not influence the DC but the α -exponents. Therefore, the α values show a richer variability than DC within this group. This may explain the absence of a negative correlation between DC and α for group 2A.

Pereda et al. (1998) reported a similar correlation between the spectral exponent β and DC regarding the overall behavior over all sleep stages. The spectral exponent β is related to the self-similarity exponent α (see Section 2.3). However, considering single sleep stages they found strongest correlations in REM sleep, waking and stage 1. This difference to our findings may result from the small number of segments analyzed by Pereda et al. (1998) or from the different algorithms used.

The dominant influence of delta power P_δ on DC, together with the fact that the self-similarity exponent is strongly correlated with the delta power, verified primarily the crucial role of delta power in the analysis of the sleep EEG. Concerning power in the other spectral bands, i.e. P_θ , P_α and P_σ , we found only for P_α an independent influence on DC: the stronger the power P_α the higher the dimension. This correlation exists, however, only in slow-wave sleep while the overall behavior shows a negative correlation between alpha power and DC. It was observed in two subjects who exhibited pronounced alpha activity in slow-wave sleep in addition to stochastic background activity, and might be related to alpha-delta sleep (Pivik and Harman, 1995). This was the only result, however, which was not consistent for all 4 subjects. The background activity produced negative correlations but the alpha waves were responsible for positive correlations. These findings suggest to parameterize the spectrum as a background part, described by a power law with the exponent β and spectral peaks of rhythmic activity such as slow waves, alpha waves, theta oscillations or sleep spindles.

It should be noted that our analysis is based on a single derivation, i.e. univariate data. A generalization to the multivariate case (multiple derivations) needs further investigation.

In summary, our analysis demonstrated that the dimen-

sional complexity of the sleep EEG reflects both linear and nonlinear features. The interplay between linear and nonlinear aspects in DC might be advantageously employed for diagnostics or classification purposes in such cases, in particular if both effects act in the same direction. This seems to be the case in EEG from epileptic patients. Interictal EEG from epileptic patients showed increased power in lower frequencies (0.25–8 Hz) compared to higher frequencies (8.25–30 Hz) (Drake et al., 1998). Our results suggest that this leads to a decrease of both DC and $\langle DC^{\text{sur}} \rangle$. Moreover, it is known that interictal EEG of epileptic patients exhibits nonlinear signatures in DC, which leads to an additional decrease of DC compared to $\langle DC^{\text{sur}} \rangle$ (Lehnertz and Elger, 1995).

For the purpose of a better understanding of the underlying processes, however, this interplay of linear and nonlinear features renders the use of the dimensional complexity ambiguous, because changes in DC might have very different origins. In particular our results suggest that one should first check whether differences in DC are caused by changes in the linear properties of the signal before advocating more ambitious interpretations.

Acknowledgements

We thank R. Badii and R. Füchslin for fruitful discussions and H.P. Landolt for comments on the manuscript. This work was supported by the Helmut Horten Stiftung, the Swiss National Science Foundation and the University of Zurich.

Appendix A. Automatic algorithm for DC determination

First the EEG segments were filtered by a 8th-order low-pass Butterworth filter (−3 dB at 30 Hz). For the estimation of DC we used an automatic plateau detection algorithm proposed by Schmid and Dünki (1996).

The correlation sum (see Eq. (1)) was calculated at a set of length scales with $\ln(r_i/r_{i+1}) = 0.05$ using the embedding parameters $(m, r, W) = (20, 3\Delta, 1\Delta)$ as described in Section 2.2. $D_2(r_i)$ is estimated by fitting the slope of $\ln C(r)$ vs. $\ln(r)$ for 5 neighboring points centered at r_i . Subsequently, the scaling regions $[r_{\min}, r_{\max}]$ called plateaus, in which $D_2(r_i)$ remains approximately constant, are searched in the $D_2(r_i)$ curve. A plateau should fulfill the following three criteria:

1. The slope s of a plateau candidate and its 95% confidence interval is calculated by fitting a straight line to the data points $(\ln(r_i), D_2(r_i))$ for length scales $r_{\min} \leq r_i \leq r_{\max}$. The value $s = 0$ must lie within the confidence interval.
2. The so-called flatness $F = |D_2^{\max} - D_2^{\min}|/D_2^{\max}$ is calculated for this plateau candidate. The value of F must be less than a predefined threshold value, which we set to 0.15.
3. The length of a plateau candidate $R = \ln(r_{\max}/r_{\min})$ must be

larger than or equal to a predefined value $R \geq 0.2$. The plateau with the largest R value will be taken for DC-determination. If there is more than one plateau with the same maximal value of R the one with the smallest flatness F is used.

Finally, the DC value is determined by fitting the slope of $\ln C(r)$ vs. $\ln(r)$ in the scaling region where we find the optimal plateau.

In practice the algorithm starts with the largest possible R and reduces it stepwise until an acceptable plateau is found. If no such plateau is found for a segment, this segment is excluded from further analysis. For the surrogate data analysis we had to modify this rule, because we had to attribute each surrogate data segment a DC value. Therefore, if no DC could be estimated using the conditions given above, we considered intervals with $R = 0.15$ and chose the plateau with the smallest value of F to estimate a DC value for this surrogate data segment.

The values of the parameters F and R have to be determined as a tradeoff between the quality of the plateau and the probability for finding a plateau. The latter determines whether there is a sufficiently large amount of segments for further statistical analysis.

Appendix B. Self-similar time series and detrended fluctuation analysis

A time series $x(t)$ is self-similar when a scaling in the t -direction by a factor b requires a rescaling in the x -direction by a factor b^{H_2} to preserve the statistical properties in the rescaled graph. Here, H_2 is the so-called Hurst exponent. The H_2 exponent describes the roughness of the time series. A variety of methods can be used to estimate H_2 exponents. For instance, the H_2 value can be determined from a power-law spectrum, since the spectral exponent β is related to H_2 by $\beta = 2H_2 + 1$.

A recent method, known as detrended fluctuation analysis (DFA) (Peng et al., 1994), is used to determine the self-similarity exponent α , which is related to H_2 by $\alpha = H_2 + 1$. While this relation is restricted to fractional Brownian motion, i.e. $\alpha \geq 1$, the DFA can be also applied to fractional Gaussian noise, a stochastic processes with power law spectrum and $-1 \leq \beta \leq 1$ or $0 \leq \alpha \leq 1$ (cf. Eq. (5)).

First, for a time series $\{x_i\}$ of length N , one constructs the running sum

$$y(n) = \sum_{k=1}^n x_k \quad (n = 1, \dots, N)$$

the so-called profile. Second, one divides the profile into windows of size t . In order to obtain better statistics, a sliding window (Buldyrev et al., 1995) approach has been used. Third, one determines the best linear fit of the profile in each window y , $y_i(n) = a \cdot n + b$. Finally, one defines the fluctua-

tion function as

$$F(t) = \sqrt{\frac{1}{N-t+1} \cdot \sum_{i=0}^{N-t} \left(\frac{1}{t+1} \cdot \sum_{n=1}^{i+t} [y(n) - y_i(n)]^2 \right)} \quad (A1)$$

The value of $F^2(t)$ can be considered as the error of the approximation of $y(n)$ by a smooth function with resolution of scale t (Viswanathan et al., 1997). For a self-similar time series, the fluctuation function $F(t)$ scales with t as

$$F(t) \propto t^\alpha \quad (A2)$$

In the first-order DFA, linear trends in the profile and therefore trends of zero order, i.e. moving average, in the original data are eliminated. To remove also the trends of first order, i.e. linear trends, in the original data, we determine the best quadratic fit of the profile (Bunde et al., 2000) in each window i , $y_i(n) = a \cdot n^2 + b \cdot n + c$. According to Eq. (A1), the standard deviation of the differences between the profile and these parabola is given by the fluctuation function.

References

- Achermann P, Borbély AA. Low-frequency (< 1 Hz) oscillations in the human sleep electroencephalogram. *Neuroscience* 1997;81:213–222.
- Achermann P, Hartmann R, Gunzinger A, Guggenbühl W, Borbély AA. All-night sleep EEG and artificial stochastic control signals have similar correlation dimensions. *Electroenceph clin Neurophysiol* 1994a;90:384–387.
- Achermann P, Hartmann R, Gunzinger A, Guggenbühl W, Borbély AA. Correlation dimension of the human sleep electroencephalogram: cyclic changes in the course of the night. *Eur J Neurosci* 1994b;6:497–500.
- Babloyantz A, Salazar JM, Nicolis C. Evidence of chaotic dynamics of brain activity during the sleep cycle. *Phys Lett A* 1985;111:152–156.
- Besthorn C, Sattel H, Geigerkabisch C, Zerfass R, Forstl H. Parameters of EEG dimensional complexity in Alzheimers disease. *Electroenceph clin Neurophysiol* 1995;95:84–89.
- Buldyrev SV, Goldberger AL, Havlin S, Mantegna RN, Matsu ME, Peng C-K, Simons M, Stanley HE. Long-range correlation properties of coding and noncoding DNA sequences: Genbank analysis. *Phys Rev E* 1995;51:5084–5091.
- Bunde A, Havlin S, Kantelhardt JW, Penzel T, Peter J-H, Voigt K. Correlated and uncorrelated regions in heart-rate fluctuations during sleep. *Phys Rev Lett* 2000;85:3736–3739.
- Drake ME, Pamadan H, Newell SA. Interictal quantitative EEG in epilepsy. *Seizure* 1998;7:39–42.
- Ehlers CL, Havstad JW, Garfinkel A, Kupfer DJ. Nonlinear analysis of EEG sleep states. *Neuropsychopharmacology* 1991;5:167–176.
- Elger CE, Lehnertz K. Seizures prediction by evidence non-linear time series analysis of brain electrical activity. *Eur J Neurosci* 1998;10:786–789.
- Endo T, Roth C, Landolt H-P, Werth E, Aeschbach D, Achermann P, Borbély AA. Selective REM. sleep deprivation in humans: effects on sleep and sleep EEG. *Am J Physiol* 1998;274:R1186–R1194.
- Fell J, Röschke J, Beckmann P. Deterministic chaos and the first positive Lyapunov exponent: a nonlinear analysis of the human electroencephalogram during sleep. *Biol Cybern* 1993;69:139–146.
- Fell J, Röschke J, Mann K, Schafer C. Surrogate data analysis of sleep electroencephalograms reveals evidence for nonlinearity. *Biol Cybern* 1996;75:85–92.
- Ferri R, Parrino L, Smerieri A, Terzano MC, Elia M, Musumeci SA, Pettinato S, Stam CJ. Non-linear EEG measures during sleep: effects of the

- different sleep stages and cyclic alternating pattern. *Int J Psychophysiol* 2002;43:273–286.
- Grassberger P, Procaccia I. Characterization of strange attractors. *Phys Rev Lett* 1983a;50:346–349.
- Grassberger P, Procaccia I. Measuring the strangeness of strange attractors. *Physica D* 1983b;9:189–208.
- Kantz H, Schreiber T. *Nonlinear time series analysis*, Cambridge: Cambridge University Press, 1997.
- Kugiumtzis D. Test your surrogate data before you test for nonlinearity. *Phys Rev E* 1999;60:2808–2816.
- Lehnertz K, Elger CE. Spatio-temporal dynamics of the primary epileptogenic area in temporal lobe epilepsy characterized by neuronal complexity loss. *Electroenceph clin Neurophysiol* 1995;95:108–117.
- Osborne AR, Provenzale A. Finite correlation dimension for stochastic systems with power-law spectra. *Physica D* 1989;35:357–381.
- Peng C-K, Buldyrev SV, Havlin S, Simons M, Stanley HE, Goldberger AL. Mosaic organization of DNA nucleotides. *Phys Rev E* 1994;49:1685–1689.
- Pereda E, Gamundi A, Rial R, Gonzalez J. Non-linear behaviour of human EEG: fractal exponent versus correlation dimension in awake and sleep stages. *Neurosci Lett* 1998;250:91–94.
- Pivik RT, Harman K. A reconceptualization of EEG alpha activity as an index of arousal during sleep: all alpha activity is not equal. *J Sleep Res* 1995;4:131–137.
- Pradhan N, Sadasivan P, Chatterjji S, Dutt DN. Patterns of attractor dimensions of sleep EEG. *Comput Biol Med* 1995;25:455–562.
- Press WH, Teukolsky SA, Vetterling WT, Flannery BP. *Numerical recipes in C*, Cambridge: Cambridge University Press, 1992.
- Pritchard WS, Duke DW. Measuring chaos in the brain: a tutorial review of nonlinear dynamical analysis. *Int J Neurosci* 1992;67:31–80.
- Rapp PE, Albano AM, Schmah TI, Farwell LA. Filtered noise can mimic low dimensional chaotic attractors. *Phys Rev E* 1993;47:2289–2297.
- Rechtschaffen A, Kales A. *A manual of standardized terminology, techniques and scoring system for sleep stages of human subjects*, NIH Publication, no. 204. Washington, DC: Public Health Services, NIH, 1968.
- Rey M, Guillemant P. Apport des mathématiques non-linéaires (théorie du chaos) à l'analyse de l'EEG. *Neurophysiol Clin* 1997;27:406–428.
- Röschke J, Aldenhoff J. The dimensionality of human's electroencephalogram during sleep. *Biol Cybern* 1991;64:307–313.
- Schmid CB, Düñki RM. Indications of nonlinearity, intraindividual specificity and stability of human EEG: The unfolding dimension. *Physica D* 1996;93:165–190.
- Schreiber T. Interdisciplinary application of nonlinear time series methods. *Phys Rep* 1999;308:2–64.
- Schreiber T, Schmitz A. Improved surrogate data for nonlinearity tests. *Phys Rev Lett* 1996;77:635–638.
- Schreiber T, Schmitz A. Surrogate time series. *Physica D* 2000;142:346–382.
- Theiler J. Spurious dimensions from correlation algorithms applied to limited time-series data. *Phys Rev A* 1986;34:2427–2432.
- Theiler J, Prichard D. Using 'surrogate surrogate data' to calibrate the actual rate of false positives in tests for nonlinearity in time series. In: Cutler CD, Kaplan DT, editors. *Nonlinear dynamics and time series*, Fields Institute communications, vol. 11. Providence, RI: American Mathematics Society, 1997. pp. 99–113.
- Theiler J, Rapp PE. Re-examination of the evidence for low-dimensional, nonlinear structure in the human electroencephalogram. *Electroenceph clin Neurophysiol* 1996;98:213–222.
- Theiler J, Eubank S, Longtin A, Galdrikian B, Farmer JD. Testing for nonlinearity in time series: the method of surrogate data. *Physica D* 1992;58:77–94.
- Tirsch WS, Keidel M, Perz S, Scherb H, Sommer C. Inverse covariation of spectral density and correlation dimension in cyclic EEG dynamics of the human brain. *Biol Cybern* 2000;82:1–14.
- Viswanathan C, Buldyrev S, Havlin S, Stanley H. Quantification of DNA patchiness using long-range correlation measures. *Biophys J* 1997;72:866–875.